PERGAMON

International Journal of Solids and Structures 36 (1999) 4289–4315

INTERNATIONAL JOURNAL OF SOLIDS and STRUCTURES

Constitutive equations for polycrystalline thermoelastic shape memory alloys. Part I. Intragranular interactions and behavior of the grain

N. Siredey[a,*], E. Patoor[b], M. Berveiller[b], A. Eberhardt[a]

[a] *LPMM-ISGMP/ENIM, Ile du Saulcy, 57042 Metz Cedex 1, France*
[b] *LPMM-ISGMP/ENSAM, Ile du Saulcy, 57042 Metz Cedex 1, France*

Received 12 December 1997; in revised form 13 June 1998

Abstract

A micromacro thermomechanical modelization of grain behavior of a polycrystalline shape memory alloy is presented. This model, based on thermodynamical approach and identification of stress sources, takes into account experimental observations of the transformation microstructure. Because plates of martensite are usually observed to appear in domains, similar to subgrains, we show that determination of average global fraction of martensite is not sufficient to describe grain behavior. A better approximation is done by taking an average fraction of martensite in each domain as internal variables. With these parameters a full description of evolution of material can be made. We point out that free energy of the material depends on an interaction matrix between martensites. Moreover the calculation of this matrix for CuAlBe alloys allows one to determine the interface between domains. The results of this study are used to model the whole behavior of the polycrystalline material with a self-consistent method.

1. Introduction

The thermomechanical behavior of solids undergoing martensitic transformation has been studied for many years. These materials may be divided into two classes according to the presence of plastic flow (Cohen et al., 1979; Christian et al., 1995):

- in Shape Memory Alloys (SMA), no (or negligible) plastic flow occurs and the main mechanism corresponds to the formation of martensitic plates with given eigenstrains. The elastic behavior of both phases is nearly the same;
- in the case of Transformation Induced Plasticity (TRIP), internal stresses are related with the

* Corresponding author

0020-7683/99/$ - see front matter
PII: S0020-7683(98)00196-6

transformation and induce plastic flow of the parent phase which in turn modifies the transformation conditions. In addition, the plastic behavior of such a two phase material appears highly heterogeneous since, in that case, the yield stress of the product phase (martensite) is several times higher than that of austenite.

SMA polycrystals present special industrial interest because of their subsequent superthermoelasticity (Krishnan et al., 1974) and so have been studied by many authors. To model their behavior, various approaches have been used. At the microscopic level, James et al. (Chu and James, 1995; Abeyaratne et al., 1996) have extended the concept of Weschler et al. (1953) to more complex transformation microstructures corresponding to minima of the free energy. In that case, the polycrystalline aspect is ignored and dissipation is not allowed so that some aspects of the overall behavior is not reproduced. The thermomechanical behavior may also be obtained in the framework of Generalized Standard Materials using the average volume fraction of martensite and the mean transformation strain over the volume of martensite as internal variables; see for example, Bekker and Brinson (1997), Boyd and Lagoudas (1996), Delobelle and Lexcellent (1996), Falk (1980), Leclercq and Lexcellent (1996), Müller and Xu (1991), Peyroux et al. (1996), Raniecki and Lexcellent (1994), Sittner et al. (1996), Stalmans et al. (1995), Tanaka et al. (1986). In that case, some difficulties occur to account for the interaction energy between austenite and martensite and the determination of the evolution of the mean transformation strain becomes complicated. In that case, the fluctuations of the transformation strain field inside the martensite are not taken into account. Micromechanical studies starting at the level of the martensitic plate where the transformation strain may be taken as uniform, associated with scale transition theories, have been more successfully applied to shape memory alloys using a two-phase approach (Sun and Hwang, 1991) or, for a single crystal, using Mori–Tanaka scheme (Sun and Hwang, 1994). In both cases, the polycrystalline microstructure is absent and in the case of Sun and Lexcellent (1996), the variant–variant interaction model does not allow spatial organization of the transformation microstructure nor accommodation by orientation of the variant–variant interfaces. Polycrystalline and texture effects are accounted by Bhattacharyan (1996) with a purely kinematical point of view considering the change of symmetry that is produced during the transformation from austenite to martensite. This approach is able to determine the polycrystalline recoverable strain but no information is given on the overall behavior, in addition a stress free microstructure is assumed inside each grain. In a previous study, Patoor et al. (Entemeyer et al., 1995) use a self-consistent model for the polycrystalline problem and an interaction matrix for the variant interactions allowing some self organization of the transformation microstructure. However this matrix needs experimental identification of some material parameters.

For a polycrystalline Representative Volume Element (RVE) the overall behavior strongly depends on material free energy composed of (Wollants et al., 1979; Warlimont, 1976):

- a chemical part due to the lattice change related to the phase transformation;
- an interfacial term associated with the creation of interfaces between austenite and martensite. This part is usually negligible for classical SMA;
- an elastic part related to imposed boundary conditions and internal stresses associated with inter- and intragranular incompatibilities of the transformation strain field.

Grain boundaries are obstacles for the expansion of martensitic plates over the RVE so that

interactions between transforming grains lead to the development of stress and strain fluctuations at the grain scale. The resolution of such a problem has been examined for elastic–plastic polycrystals (Lipinski and Berveiller, 1989). The self consistent model developed in this context will be recalled in Part II and extended to SMA.

Inside the grains, stress and strain fluctuations also appear due to the formation of a transformation microstructure. The shape of the elementary transformed volume corresponds generally to a thin plate. Moreover, for the whole microstructure, one has to take into account the spatial distribution of these plates and their local interactions. Contrary to grain boundaries, the interfaces related with transformation (austenite–martensite and martensite–martensite interfaces) are highly mobile and must be considered as internal variables describing the transformation microstructure.

The overall thermomechanical behavior of a grain is clearly sensitive to these two microstructural levels: plate scale and spatial distribution of plates. Nevertheless for modelling a simplified representation of the changing microstructure has to be introduced. From both a pure kinematical approach and the expression of the free energy, the volume fractions of each variant $n\{f_n, n = 1\text{–}24\}$ appear as the adequate set of internal variables for the description of the martensitic transformation as well as for that of the reorientation mechanism (Patoor et al., 1987).

The derivation of the thermomechanical constitutive relation of the single crystal embedded in the polycrystal follows from classical approach in the framework of thermodynamics of irreversible processes since creation (or shrinkage) of martensitic plates proceeds with (low) intrinsic dissipation as observed on single crystal experiments. These experiments (Grujicic et al., 1985; Buathier, 1995) show two types of growing of martensite area. In well prepared single crystal, the transformation is related with the motion of a single interface between austenite and martensite corresponding to the growing of a single plate. In that case, the interfacial motion is thermally activated and lies between 10^{-6} and 10^{-2} m/s. When more than one nucleation site exists (in ordinary single crystals or polycrystals) the transformation progresses by creation of new plates. Then the direct or reverse transformation proceeds quasi instantaneously (plates are formed with near sound velocity), the framework of time independent inelasticity seems to be appropriate (Rice, 1971).

In that case, the driving force on an internal variable (here $\{f_n\}$) has to reach a critical value before transformation takes place. This is equivalent to introduce a dissipation potential. In the first part of this paper, the observed transformation microstructures are presented and analysed in terms of incompatibilities considered as sources of internal stresses. In the most common case, the observed microstructure corresponds to the formation of several domains such as subgrains in which only one variant seems to be activated. The boundaries between these domains have to be described by additional internal variable X_i. In the second part, the free energy is decomposed into two terms depending only on the loading parameters (E, T) and the set of volume fractions of martensite variants $\{f_n\}$, and a third term depending on the whole transformation strain field with internal variables $(X_i, \{f_n\})$. This last term is developed for a microstructure with domains and the additional internal variables (X_i) are deduced from the minimization of the corresponding free energy term. Since the remaining internal variables are linked together by the definition of the volume fractions $(0 \leqslant \sum_n f_n \leqslant 1)$, the related physical constraints are taken into account using the Kuhn–Tucker conditions in the derivation of the corresponding driving forces. This allows one to find, in a classical way, the evolution of the internal variables $\{f_n\}$ and the corresponding overall response for the grain. The model leads to an interaction matrix between variants and will be applied to a CuAlBe alloy.

In chapter 6, experimental results on CuAlBe single crystals are presented and used to identify the material parameters introduced during the modelization.

2. Different transformation microstructures observed for stress induced martensitic phase transformation

Tensile tests were performed on polycrystalline CuAlBe wires. Figure 1 presents the evolution of stress assisted martensitic transformation during loading (Buathier, 1995). One can note that phase transformation occurs inside grains with non randomly spatial distribution. In fact, two types of martensitic plates arrangement can be distinguished in each grain.

2.1. Morphology A

The first plates distribution is shown in the area A and is the most common feature. A grain is divided into substructures named domains. Each domain of volume V_n and boundary ∂V_n is defined as a mixture of untransformed matrix and parallel plates of martensite corresponding to the activation of only one variant. Other variants encountered in the grain stand mainly in other domains. During loading, phase transformation proceeds with creation of new plates of one or more variants; however these new variant plates stay in the previous domain. Three scales of interfaces, where incompatibilities and hence sources of stresses exist, can be determined.

(1) Inside domain interfaces have to accommodate lattice differences between austenite and martensite. This is actually realized by martensitic transformation itself, as it does not differ in this material from that obtained from the Weschler et al. theory (1953). This result was emphasized by El Amrani Zirifi (1994) in a nearly identical material: CuZnAl alloy. He found that, for this material where thermoelastic martensite also exists, and with the hypothesis of very few plasticity, homogeneous and isotropic elasticity, no temperature effect, W.L.R. strain transformation field ε^T fills quite well compatibilities conditions. These were given by Kröner (1980) as

$$Inc\,\varepsilon^T = \eta \tag{1}$$

which, in the case of a piecewise uniform transformation strain field, leads to

$$Inc\,\varepsilon^T_{ij} = -\epsilon_{ikm}\epsilon_{jln}\varepsilon^T_{mn}n_k n_l = \eta_{ij} \tag{2}$$

where ϵ_{ijk} is the permutation tensor, n_j the unit normal to the interface and η the incompatibility tensor. The condition of compatibility is then

$$\eta = 0 \tag{3}$$

The condition of compatibility is automatically satisfied if **n** is the normal to the habit plane.

The interface corresponding to the habit plane between martensite and matrix can thus be considered as compatible and no stress sources are produced there.

(2) Plates of martensite are not infinite and their tips lie in the domain boundaries. Moreover, at this place, plates of martensite of one domain meet either plates of another variant of the other domain or grain boundaries. So, interfaces between domains have to accommodate different

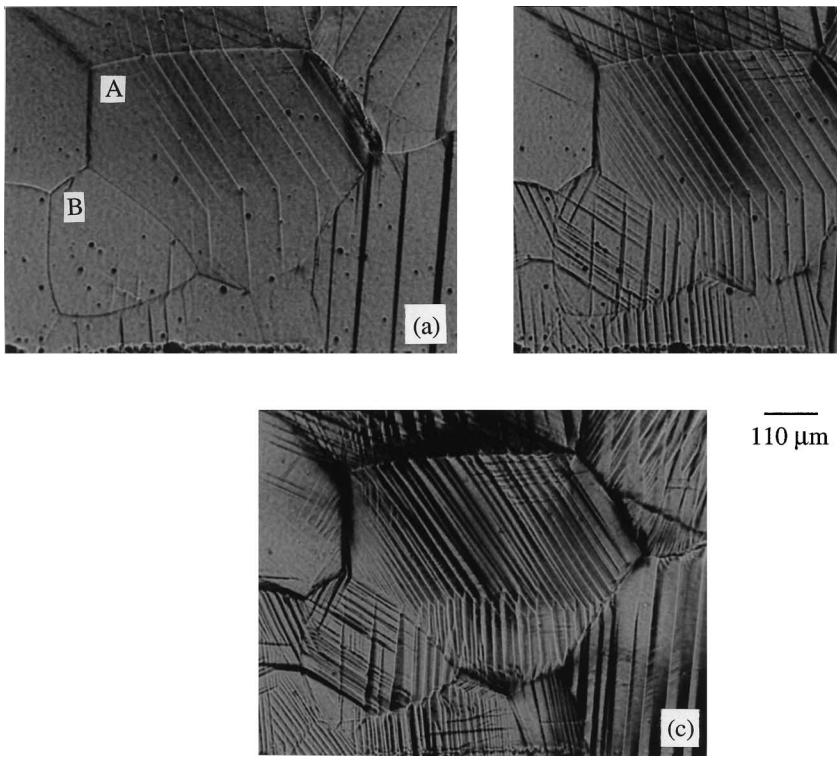

Fig. 1. Various photographs taken during a tensile test of a polycrystalline 11.5 wt%Al–0.5 wt%Be–Cu alloy at room temperature and showing the evolution of plates of martensite in two grains: A and B. Strain is (a) 0.71%, (b) 1.69%, (c) 4.11%.

transformation strains. It is reasonable to expect from this situation some possible incompatibilities. These incompatibilities will induce internal stresses and contribute to the free energy of the material.

Due to the characteristics of martensitic transformation, interfaces appear as a type of quasi-dislocation wall. Then, at this scale, the domain frontier presents fluctuations due to stacking of martensite and matrix areas. Near the interface, the stress field should present such fluctuations. On the other hand, as for the case of stresses created by infinite or limited dislocation walls, we assume that fluctuations reduce far from the interface and the stress field due to incompatibility becomes more uniform. Such an interface between domains is able to move according to the external loading or to the internal stresses and will be another degree-of-freedom for the transformation microstructure.

(3) Finally one has to take into account the meetings of domains or plates of martensite with grain boundaries. These are expected to be other incompatible interfaces whose main characteristics are to be given, at the opposite of domain boundaries inside a grain. At a more macroscopic point of view, this phenomenon can be viewed as part of the problem of intergranular accommodation during loading. For that reason, these sources of stress can be treated with the self-consistent method applied to polycrystalline material which will be developed in Part II.

For single crystal study, the only incompatibilities to be taken into account are the ones created at the domain boundaries; their modelization will be the aim of Part I.

2.2. Morphology B

The second observed morphology or martensitic transformation is presented in area B of Fig. 1. Plates of two variants of martensite cross each other. Special attention has to be paid to the meeting region where some striated features occur as a consequence of a tentative of accommodation. During transformation, energy is then stored inside these regions whose precise description has to be done for complete modelization.

2.3. Discussion

One can see from experiments that third order internal stresses are clearly dependent of the intragranular substructure, not only in terms of shape, orientation and crystallography for each variant plate, but also in terms of spatial distribution of these plates. As the thermomechanical behavior of material depends strongly on internal stresses, the models need to take into account these substructures.

A classical way to solve the problem of thermomechanical behavior of composite material is to use Eshelby–Kröner or Kröner/Mori–Tanaka approaches (Mura, 1993). These types of models are based on inclusions of phase 2 (e.g. martensite) embedded in a matrix phase. For morphology A, this approach cannot be used directly, since each plate of martensite is considered as a unique inclusion inside a corrected matrix with uniform transformation strain. This is the case neither for morphology A nor B. Moreover no spatial correlations should exist between inclusions: this excludes the reorientation mechanism between variants commonly observed. Finally inclusion distribution does not appear in the model which (implicitly) assumes a disordered substructure. Thus, a specific micromechanical model has to be developed in order to take into account the transformation microstructures.

Such an approach, also based on Eshelby–Kröner and Mori–Tanaka model, considers as inclusions not the plates themselves but domains of volume V_n as defined in the case of morphology A: mixture of matrix and plates of one variant of martensite. Such an approach has been developed in the previous studies of Patoor et al. (Entemeyer et al., 1995; Entemeyer, 1996; Patoor et al., 1996, 1997) presented in the Introduction. They show that, with respect to classical models of Delobelle and Lexcellent (1996) or Stalmans et al. (1995) some additional internal parameters should be taken into account. These parameters are related to the set of $\{f_n\}$. These variables can be obtained from experimental measurements and then no fitting parameters are required. On the other hand, minimization of energy for surface orientation between inclusions and surrounding—constituted by another domain—is made. Using the self-consistent approach, the model has been applied to uniaxial loadings of polycrystals. The obtained results agree quite well with experiments.

This model still requires some input parameters obtained from metallurgical observations. The model developed here, based on a thermodynamical study of energy created by incompatibilities at the boundary domains will attempt to be released from these types of input data.

In the case of morphology B, the modelization of internal sources of energy needs a detailed description of the crossing of martensitic plates. This complex problem will not be discussed in the frame of this study.

3. Free energy related to martensitic transformation in a grain

In this part, we consider a grain with volume V and boundary ∂V as a representative volume element (RVE). The stress free austenite matrix is considered as the reference state. Thermal strains and thermomechanical coupling are neglected and homogeneous elasticity is assumed.

When transformation occurs, some parts v_i ($i = 1$–N) of V undergo uniform transformation strains ε^{Ti}. The field $\varepsilon^T(r)$ is called the transformation strain field. From experimental crystallographic measurements and data on invariant lattice transformation, the Wechsler et al. (1953) phenomenological theory allows one to determine the characteristics of this transformation. By this way, it is possible to forecast orientation relations between matrix and martensite, habit plane normal $\mathbf{n}'$, displacement direction $\mathbf{m}$ and displacement magnitude g, illustrated in Fig. 2. The transformation strain is then expressed for a typical variant by

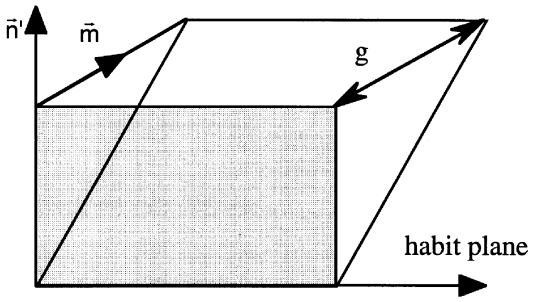

Fig. 2. Deformation of a matrix volume element into a martensitic one.

$$\varepsilon_{ij}^{T} = \tfrac{1}{2}(m_i n'_j + m_j n'_i)g \tag{4}$$

For the sake of symmetry of matrix crystalline lattice, many equivalent systems are implied in martensitic transformation. There are 24 of these so-called variants in CuAlBe alloys.

It is assumed that the transformation strain field is piecewise uniform, corresponding to one given value of the transformation strain over the whole volume of each martensitic plate and being zero inside the matrix.

The free energy of the austenite–martensite system results from:

- the elastic strain energy with density $\omega(r)$,

$$\omega(r) = \tfrac{1}{2}\sigma_{ij}(r)\varepsilon_{ij}^{e}(r) \tag{5}$$

  σ is the local stress field created by the loading conditions on ∂V and by the incompatibilities of the ε^T field;
- the crystallographic (or chemical) free energy with density $\varphi(r)$;
- the interfacial energy related with austenite–martensite interfaces as well as martensite–martensite ones. These last terms are usually neglected in the case of thermoelastic shape memory alloys.

Other sources of free energy (points defects, dislocations,...) are neglected and the thermomechanical loading process is assumed to be slow enough so that the temperature remains uniform over the RVE.

For a unit volume V, the free energy Φ is given by

$$V\Phi = \int_V \omega(r)\,\mathrm{d}r + \int_V \varphi(r)\,\mathrm{d}r \tag{6}$$

Since $\varphi(r)$ is uniform in the austenite ($=\varphi_A$ over the volume V_A) and uniform inside the martensite ($=\varphi_M$ over the volume V_M), the second term in eqn (6) may be written as

$$\int_V \varphi(r)\,\mathrm{d}r = V_A \cdot \varphi_A(T) + V_M \cdot \varphi_M(T) \tag{7}$$

so that

$$\frac{1}{V}\int_V \varphi(r)\,\mathrm{d}r = f \cdot \varphi_M(T) + (1-f)\cdot \varphi_A(T) \tag{8}$$

$$= \varphi_A(T) + (\varphi_M - \varphi_A) f \tag{9}$$

where $f = (V_M/V)$ is the total volume fraction of martensite.

In the vicinity of the equilibrium temperature T_0 where $\varphi_A = \varphi_M$, the chemical part of the free energy is usually linearized by

$$\frac{1}{V}\int_V \varphi(r)\,\mathrm{d}r = B(T - T_0) f \tag{10}$$

where B and T_0 are material parameters.

The elastic part of the free energy

$$W = \frac{1}{2V}\int_V \sigma_{ij}(r)\varepsilon^{\mathrm{e}}_{ij}(r)\,\mathrm{d}r \tag{11}$$

may be transformed using kinematical conditions inside V:

$$\varepsilon_{ij}(r) = u_{(i,j)}(r) = \varepsilon^{\mathrm{e}}_{ij}(r) + \varepsilon^{T}_{ij}(r) \tag{12}$$

and boundary conditions on ∂V:

$$u_i = E_{ij}x_j \tag{13}$$

From (11) and (12),

$$W = \frac{1}{2V}\int_V \sigma_{ij}(r)[u_{i,j}(r) - \varepsilon^{T}_{ij}(r)]\,\mathrm{d}r \tag{14}$$

By partial integration and taking into account boundary conditions (13), (14) is reduced to

$$W = \frac{1}{2}\Sigma_{ij}E_{ij} - \frac{1}{2}\int_V \sigma_{ij}(r)\varepsilon^{T}_{ij}(r)\,\mathrm{d}r \tag{15}$$

where

$$\Sigma_{ij} = \frac{1}{V}\int_V \sigma_{ij}(r)\,\mathrm{d}r \tag{16}$$

represents the overall stress.

We decompose the stress σ into the macroscopic stress Σ and the internal stress τ (only related with the ε^T field):

$$\sigma = \Sigma + \tau \tag{17}$$

so that

$$\tau_{ij,j}(r) = 0 \tag{18}$$

and

$$\frac{1}{V}\int_V \tau_{ij}(r)\,\mathrm{d}r = 0 \tag{19}$$

Using uniform elasticity with moduli C, (15) is written as

$$W = \frac{1}{2}(E_{ij} - E^{T}_{ij})C_{ijkl}(E_{kl} - E^{T}_{kl}) - \frac{1}{2V}\int_V \tau_{ij}(r)\varepsilon^{T}_{ij}(r)\,\mathrm{d}r \tag{20}$$

where

$$E^{T}_{ij} = \frac{1}{V}\int_V \varepsilon^{T}_{ij}(r)\,\mathrm{d}r \tag{21}$$

represents the overall transformation strain and the second term of (20) is only related with the transformation strain field $\varepsilon^T(r)$.

Since ε^T is uniform over the different martensitic domains v_n, one has

$$E_{ij}^T = \sum_n \varepsilon_{ij}^{Tn} f_n \quad \left(f_n = \frac{v_n}{V}\right) \tag{22}$$

and for the chemical energy:

$$B(T-T_0)f = B(T-T_0)\sum_n f_n. \tag{23}$$

Finally, the Helmholtz global free energy Φ depends on control parameters $\{E, T\}$ and transformation field $\{\varepsilon^T\}$. Its expression,

$$\Phi(E, T, \{\varepsilon^T\}) = \frac{1}{2}(E_{ij}-E_{ij}^T)C_{ijkl}(E_{kl}-E_{kl}^T) + B(T-T_0)\sum_n f_n - \frac{1}{2V}\int_V \tau_{ij}(r)\varepsilon_{ij}^T(r)\,\mathrm{d}r \tag{24}$$

or

$$\Phi(E, T, \{\varepsilon^T\}) = \frac{1}{2}(E_{ij}-E_{ij}^T)C_{ijkl}(E_{kl}-E_{kl}^T) + B(T-T_0)\sum_n f_n - \sum_n \frac{1}{2}\tau_{ij}^n \varepsilon_{ij}^{Tn} f_n \tag{25}$$

with ε^{Tn} the transformation strain for variant n defined in eqn (4), needs the determination of the mean internal stress τ^n over the volume v_n of variant n.

$$\tau_{ij}^n = \frac{1}{v_n}\int_{v_n} \tau_{ij}(r)\,\mathrm{d}r \tag{26}$$

If the elastic interaction energy W_{int}, expressed by

$$W_{\mathrm{int}} = \frac{1}{2V}\int_V \tau_{ij}(r)\varepsilon_{ij}^T(r)\,\mathrm{d}r \tag{27}$$

vanishes, the free energy Φ of V depends only on the control variables E and T and the internal variables f_n: $\Phi = \Phi(E, T, f_n)$ irrespective of the microstructure of the ε^T field.

This is obviously not the case due to the incompatibilities of the transformation strain field.

In the next part, we derive an expression for this interaction energy W_{int} for a domain type microstructure using the fact that the domain interfaces are mobile without dissipation.

4. Intragranular interactions between variants forming domains

For a given state of transformation characterized by the set of volume fraction $\{f_n\}$, the interaction energy $W_{\mathrm{int}} = (1/2V)\int_V \tau_{ij}(r)\varepsilon_{ij}^T(r)\,\mathrm{d}r$ depends on the transformation microstructure, i.e. the ε^T field as previously mentioned.

In this work we focus on the case of intragranular microstructures presented in Fig. 3 where the active variants define austenite–martensite domains. Each domain has a volume V_n and the martensite with transformation strain ε^{Tn} occupy a volume v_n. In the grain, each domain, or island, ends at grain boundary in such a way that these domains meet the other ones by only a side. This interface between two domains (n, m) is supposed to be a plane with unit normal N^{nm}. From Fig. 3 and notation previously introduced, we define:

- the volume fraction of each domain n: $F_n = (V_n/V)$ with the relation

$$\sum_n F_n = 1 \tag{28}$$

- the volume fraction of variant n over the volume V: $f_n = (v_n/V)$;
- the volume fraction of variant n inside the corresponding domain V_n:

$$\xi_n = \frac{v_n}{V_n} = \frac{f_n}{F_n} \tag{29}$$

- the mean transformation strain over V_n:

$$\bar{\varepsilon}^n_{ij} = \frac{1}{V_n}\int_{V_n} \varepsilon^{Tn}_{ij}\,\mathrm{d}V = \varepsilon^{Tn}_{ij}\frac{v_n}{V_n} = \varepsilon^{Tn}_{ij}\xi_n \tag{30}$$

- the overall mean transformation strain over V:

$$E^T_{ij} = \sum_n f_n \varepsilon^{Tn}_{ij} \tag{31a}$$

or

$$E^T_{ij} = \sum_n F_n \bar{\varepsilon}^n_{ij} \tag{31b}$$

This global transformation strain E^T can be described either by (31a) or by (31b), the last equation being more adapted for the estimation of the internal stresses. Since the interface between austenite

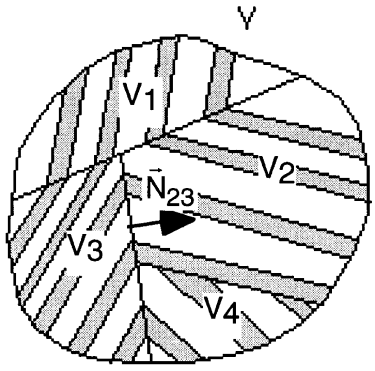

Fig. 3. Representation of the RVE showing the partition of volume V into austenite/variant i of martensite domains V_i.

and martensite inside the domains are compatible, the sources of internal stresses (and consequently of the internal energy) are located on the boundaries between domains corresponding to the tip of martensitic plates. These boundaries may be considered as quasidislocation walls with long range internal stresses.

As a consequence, the stress field fluctuates, weakly inside the domains and presents jumps across the domain interface. Therefore, it may be evaluated using interface operator techniques, with the jumps of mean transformation strain across the interfaces as sources of incompatibilities.

The interaction energy depends now on the given set of volume fractions $\{f_n\}$ and the microstructural parameters of the domains reduced to the volume fractions $\{F_n\}$ and the normal to the interface $\{N^{nm}\}$.

The progress of transformation results from creation of new plates inside domains; it may be assumed that this mechanism leads to dissipation according to the attenuation of the elastic waves related with the bursts of the plates. On the contrary, for proportional loading, one can assume that the domains microstructure evolves without dissipation so that the corresponding internal variables ($\{F_n\}, \{N^{nm}\}$) should minimize the corresponding free energy term W_{int}.

According to these assumptions the interaction energy becomes

$$W_{\text{int}} = \frac{1}{2}\sum_n f_n \varepsilon_{ij}^{Tn} \bar{\tau}_{ij}^n \tag{32}$$

where

$$\bar{\tau}_{ij}^n = \frac{1}{V_n}\int_{V_n} \tau_{ij}(r)\,\mathrm{d}r \tag{33}$$

is the mean internal stress inside the domain V_n. Using the definition of the mean transformation strain over this domain given by eqn (30), (27) may be transformed in

$$W_{\text{int}} = \frac{1}{2}\sum_n F_n \bar{\varepsilon}_{ij}^n \bar{\tau}_{ij}^n \tag{34}$$

or

$$W_{\text{int}} = \frac{1}{2}\sum_n F_n \bar{\tau}_{ij}^n \xi_n \varepsilon_{ij}^{Tn} \tag{35}$$

The relations concerning the internal stresses $\bar{\tau}^n$ are deduced from the zero mean value conditions (19)

$$\sum_n F_n \bar{\tau}_{ij}^n = 0 \tag{36}$$

and, for each interface N^{nm},

$$\bar{\tau}_{ij}^n = \bar{\tau}_{ij}^m - Q_{ijkl}^{nm}(\bar{\varepsilon}_{kl}^n - \bar{\varepsilon}_{kl}^m) \tag{37}$$

where the interface operator Q^{nm} is developed in Appendix A.

From (36) and (37), the stress inside each domain m is given by

$$\bar{\tau}_{ij}^{m} = \sum_{n} F_n Q_{ijkl}^{nm} (\bar{\varepsilon}_{kl}^{n} - \bar{\varepsilon}_{kl}^{m}) \tag{38}$$

and the interaction energy becomes

$$W_{\text{int}} = -\frac{1}{2} \sum_{m,n} F_m F_n A^{mn} \tag{39}$$

with

$$A^{mn} = \tfrac{1}{2} (\bar{\varepsilon}_{ij}^{m} - \bar{\varepsilon}_{ij}^{n}) Q_{ijkl}^{mn} (\bar{\varepsilon}_{kl}^{m} - \bar{\varepsilon}_{kl}^{n}) \tag{40}$$

Here, the following properties of Q are used:

$$Q(N) = Q(-N)$$

$$Q_{ijkl} = Q_{klij}$$

which assure the definite positivity of the A^{mn} terms.

When the transformation occurs under large applied stress (either by increasing stress at a given temperature or by cooling at a constant applied stress), experimental observations point out that mainly two principal variants grow up (Entemeyer, 1996).

In that case, the interaction energy reduces to the simplified form

$$W_{\text{int}} = -\tfrac{1}{2} F_n F_m (\bar{\varepsilon}^{n} - \bar{\varepsilon}^{m}) Q^{nm} (\bar{\varepsilon}^{n} - \bar{\varepsilon}^{m}) \tag{41}$$

which has to be minimized with respect to F_n (since $F_m = 1 - F_n$) and N^{nm}; n and m denotes the two active variants.

Using eqns (28)–(30), (41) is explicitly given by

$$W_{\text{int}} = -\frac{1}{2} F_n (1 - F_n) \left(\frac{f_n}{F_n} \varepsilon^{Tn} - \frac{f_m}{1 - F_n} \varepsilon^{Tm} \right) Q^{nm} \left(\frac{f_n}{F_n} \varepsilon^{Tn} - \frac{f_m}{1 - F_n} \varepsilon^{Tm} \right) \tag{42}$$

The derivation of W_{int} with respect to F_n leads to

$$\frac{\partial W_{\text{int}}}{\partial F_n} = -\frac{1}{2} \{ -\xi_n^2 \varepsilon^{Tn} Q^{nm} \varepsilon^{Tn} + \xi_m^2 \varepsilon^{Tm} Q^{nm} \varepsilon^{Tm} \} \tag{43}$$

whose annulation gives the condition

$$\xi_n a_n = \xi_m a_m \tag{44}$$

where

$$a_\alpha^2 = \varepsilon^{T\alpha} Q^{\alpha\beta} \varepsilon^{T\alpha} \quad (\alpha, \beta = n, m) \tag{45}$$

depends only on the unit normal to the interface between the two domains n and m.

The corresponding minimized interaction energy is now

$$W_{\text{int}} = -\frac{1}{2} f_n f_m \frac{1}{a_n a_m} (a_m \varepsilon^{Tn} - a_n \varepsilon^{Tm}) Q^{nm} (a_m \varepsilon^{Tn} - a_n \varepsilon^{Tm}) \tag{46}$$

or, introducing the interaction matrix $H^{nm} = (1/a_n a_m)(a_m \varepsilon^{Tn} - a_n \varepsilon^{Tm}) Q^{nm} (a_m \varepsilon^{Tn} - a_n \varepsilon^{Tm})$,

$$W_{\text{int}} = -\tfrac{1}{2} f_n H^{nm} f_m \tag{47}$$

Since the terms $\varepsilon^{Tm} Q^{nm} \varepsilon^{Tm}$, F_n and $(1-F_n)$ are always positive, the stability of the partial equilibrium is satisfied.

Equation (46) has to be minimized with respect to the orientation of the interface for two given variants. This can be performed numerically. It is worthwhile to point out that this matrix depends only on the elastic behavior of the material and the given set of transformation strains $\{\varepsilon^T\}$.

For CuAlBe alloys, the matrix H has been calculated and the results are discussed in Appendix B.

In the case where more than two variants are activated, we assume that the interaction energy is still described by the same type of relation so that

$$W_{\text{int}} = -\frac{1}{2} \sum_{n,m} f_n H^{nm} f_m \tag{48}$$

As discussed previously, this is an approximation of the multiple interaction between domains. Nevertheless, as it can be observed in experimental works (Entemeyer, 1996), this approximation is the best for high stress induced transformation where two principal variants are activated.

5. Expression of the free energy and behavior of a grain

Once the interaction energy term is obtained, the Helmholtz global free energy Φ per unit volume of a grain is from (24) and (48):

$$\Phi(E, T, \{f_n\}) = \frac{1}{2}(E-E^T) C (E-E^T) + B(T-T_0) f + \frac{1}{2} \sum_{n,m} H^{nm} f_n f_m \tag{49}$$

E and T are the control variables and the set $\{f_n\}$ appears as an internal variable with the physical constraints

$$f_n \geqslant 0 \quad \text{for each } n \tag{50a}$$

$$\sum_n f_n \leqslant 1 \quad \text{for the whole volume fraction} \tag{50b}$$

The overall transformation strain E^T is given by eqn (22) and $f = \sum_n f_n$. The terms C, B, T_0, ε^{Tn} and H^{nm} are material constants.

The Gibbs free energy $\Psi(\Sigma, T, \{f_n\})$ is deduced from (49) by the Legendre transformation

$$\Sigma_{ij} E_{ij} = \Phi + \Psi \tag{51}$$

so that

$$\Psi(\Sigma, T, \{f_n\}) = \frac{1}{2} \Sigma_{ij} C^{-1}_{ijkl} \Sigma_{kl} + \Sigma_{ij} E^T_{ij} - B(T-T_0) f - \frac{1}{2} \sum_{n,m} H^{nm} f_n f_m \tag{52}$$

or

$$\Psi(\Sigma, T, \{f_n\}) = \frac{1}{2}\Sigma_{ij}C^{-1}_{ijkl}\Sigma_{kl} + \sum_n \Sigma_{ij}\varepsilon^{Tn}_{ij}f_n - B(T-T_0)\sum_n f_n - \frac{1}{2}\sum_{n,m} H^{nm}f_n f_m \tag{53}$$

The physical constraints (50) are taken into account using the Kuhn–Tucker conditions in order to define the thermodynamical forces $\mathscr{F}_n$ on each volume fraction f_n.

To the $(n+1)$ conditions (50), $n+1$ Lagrange multipliers λ_0 and λ_n are introduced. They are defined by

$$\lambda_0\,(\sum_n f_n - 1) = 0 \tag{54a}$$

$$\lambda_n(-f_n - 0) = 0 \quad \text{for each } n. \tag{54b}$$

The Lagrangian $\mathscr{L}(\Sigma, T, \{f_n\})$ of the complementary free energy Ψ is defined by

$$\mathscr{L}(\Sigma_{ij}, T, \{f_n\}) = \Psi(\Sigma_{ij}, T, \{f_n\}) - \lambda_0\,(\sum_n f_n - 1) - \sum_n \lambda_n(-f_n) \tag{55}$$

The driving forces $\mathscr{F}_n$ on the volume fraction f_n is defined and given by

$$\mathscr{F}_n = \frac{\partial L}{\partial f_n} = \frac{\partial \Psi}{\partial f_n} - \lambda_0 + \lambda_n \tag{56}$$

and, from definition (53) of Ψ,

$$\mathscr{F}_n = \Sigma_{ij}\varepsilon^{Tn}_{ij} - \sum_m H^{nm}f_m - B(T-T_0) - \lambda_0 + \lambda_n \tag{57}$$

For time independent behavior, the transformation may progress on a current variant n, i.e. $\dot{f}_n \neq 0$, only if the driving force reaches a critical value $\mathscr{F}^{\mathrm{c}}_n(f_n)$ depending on the current state of transformation. This hypothesis corresponds also to the dissipation process occurring during the martensitic transformation and described by a dissipation potential W^{d}.

Now, the criteria for transformation on a variant n—$\dot{f}_n > 0$—is given by

$$\Sigma_{ij}\varepsilon^{Tn}_{ij} - \sum_m H^{nm}f_m - B(T-T_0) - \lambda_0 + \lambda_n = \mathscr{F}^{\mathrm{c}}_n \tag{58}$$

and the following conditions on the Lagrange multipliers must be satisfied:

$$\lambda_n = -\Sigma_{ij}\varepsilon^{Tn}_{ij} + \sum_m H^{nm}f_m + B(T-T_0) + \lambda_0 + \mathscr{F}^{\mathrm{c}}_n \geqslant 0 \tag{59a}$$

$$\lambda_0 = \Sigma_{ij}\varepsilon^{Tn}_{ij} - \sum_m H^{nm}f_m - B(T-T_0) + \lambda_n - \mathscr{F}^{\mathrm{c}}_n \geqslant 0 \tag{59b}$$

As soon as a variant reaches a volume fraction equal to unity or if the global volume fraction reaches one, the constraints (59) limit the transformation even if conditions (58) are satisfied.

The reverse transformation—$\dot{f}_n < 0$—may happen if the following conditions are satisfied on variant n:

$$\Sigma_{ij}\varepsilon_{ij}^{Tn}-\sum_m H^{nm}f_m-B(T-T_0)-\lambda_0+\lambda_n=-\mathscr{F}_n^{\mathrm{c}} \tag{60}$$

and Lagrange multipliers have to satisfy

$$\lambda_n=-\Sigma_{ij}\varepsilon_{ij}^{Tn}+\sum_m H^{nm}f_m+B(T-T_0)+\lambda_0-\mathscr{F}_n^{\mathrm{c}}\geqslant 0 \tag{61a}$$

$$\lambda_0=+\Sigma_{ij}\varepsilon_{ij}^{Tn}-\sum_m H^{nm}f_m-B(T-T_0)+\lambda_n+\mathscr{F}_n^{\mathrm{c}}\geqslant 0 \tag{61b}$$

Once the criterion for direct or reverse transformation rates $\dot{f}_n$ is satisfied, the coherency relation

$$\dot{\mathscr{F}}_n=\dot{\mathscr{F}}_n^{\mathrm{c}} \tag{62}$$

or here

$$\sum_{ij}\frac{\partial\mathscr{F}_n}{\partial\Sigma_{ij}}\dot{\Sigma}_{ij}+\frac{\partial\mathscr{F}_n}{\partial T}\dot{T}+\sum_m\frac{\partial\mathscr{F}_n}{\partial f_m}\dot{f}_m=\dot{\mathscr{F}}_n^{\mathrm{c}} \tag{63}$$

allows to determine the evolution of the transformation rates $\dot{f}_n$ for each variant as a function of the rate of the imposed control variables $\dot{\Sigma}$ and $\dot{T}$.

Because variants n of martensite come from symmetries in the matrix/martensite lattice change, critical forces $\mathscr{F}_n^{\mathrm{c}}$ are reasonably assumed to be identical—$\mathscr{F}_n^{\mathrm{c}}=\mathscr{F}^{\mathrm{c}}$ and since for single crystals the critical force $\mathscr{F}^{\mathrm{c}}$ is practically independent of the amount of martensite, $\dot{\mathscr{F}}^{\mathrm{c}}$ can be assumed to be zero.

In that case, (63) reduces to

$$\varepsilon_{ij}^{Tn}\dot{\Sigma}_{ij}-B\dot{T}-\sum_m H^{nm}\dot{f}_m=0 \tag{64}$$

The thermomechanical constitutive equation for the grain is defined by the relation between the overall stress rate $\dot{\Sigma}$, strain rate $\dot{E}$ and change of temperature $\dot{T}$.

From the definition (22) of E^T and Σ (16), one gets

$$\dot{\Sigma}_{ij}=C_{ijkl}(\dot{E}_{kl}-\dot{E}_{kl}^T) \tag{65}$$

or

$$\dot{\Sigma}_{ij}=C_{ijkl}\,(\dot{E}_{kl}-\sum_n\varepsilon_{kl}^{Tn}\dot{f}_n) \tag{66}$$

Multiplying (66) by ε^{Tm} yields

$$\varepsilon_{ij}^{Tm}\dot{\Sigma}_{ij}=\varepsilon_{ij}^{Tm}C_{ijkl}\,(\dot{E}_{kl}-\sum_n\varepsilon_{kl}^{Tn}\dot{f}_n) \tag{67}$$

or using (64)

$$B\dot{T}+\sum_n H^{nm}\dot{f}_n=\varepsilon_{ij}^{Tm}C_{ijkl}\,(\dot{E}_{kl}-\sum_n\varepsilon_{kl}^{Tn}\dot{f}_n) \tag{68}$$

which can be solved for $\dot{f}_n$

$$\sum_n (H^{nm} + \varepsilon_{ij}^{Tm} C_{ijkl} \varepsilon_{kl}^{Tn}) \dot{f}_n = \varepsilon_{ij}^{Tm} C_{ijkl} \dot{E}_{kl} - B\dot{T}$$

so

$$\dot{f}_n = \sum_m K^{nm} (\varepsilon_{ij}^{Tm} C_{ijkl} \dot{E}_{kl} - B\dot{T}) \tag{69}$$

where

$$K^{nm} = (H^{nm} + \varepsilon_{ij}^{Tm} C_{ijkl} \varepsilon_{kl}^{Tn})^{-1}$$

Summations are made only on the potentially active variants, i.e. those satisfying the transformation conditions (58) and (59).

Introducing (69) into (66) yields to

$$\dot{\Sigma}_{ij} = \{C_{ijkl} - \sum_{n,m} C_{ijrs} \varepsilon_{rs}^{Tn} K^{nm} \varepsilon_{pq}^{Tm} C_{pqkl}\} \dot{E}_{kl} + \sum_{n,m} C_{ijkl} \varepsilon_{kl}^{Tn} K^{nm} B\dot{T} \tag{70}$$

6. Experimental identification of material parameters

Equation (70) together with transformation conditions (58) and (59) describes the thermomechanical behavior of an austenitic grain with multivariant transformation conditions.

The material parameters appearing in (70), (58) and (59) are:

—the set of 24 transformation strains $\{\varepsilon^{Tn}\}$ from which the interaction matrix H^{nm} can be calculated;
—the elastic behavior defined by tensor C;
—the material constants related with the transformation: coefficient B, equilibrium temperature T_0 of austenite–martensite transition and critical forces for austenite–martensite transformation of each variant n: $\mathscr{F}_n^c$.

These material parameters needed for the determination of the behavior of the single crystal are deduced from the crystallographic theory of martensitic transformation and from experimental tensile tests at constant temperature or cooling tests at constant stress.

Since the elastic behavior is assumed identical for both phases, the approximation of isotropic temperature independent elasticity may be adopted. In that case the shear modulus μ and Poisson's ratio v are measured during the elastic loading of the austenite.

The crystallography of the martensitic transformation for CuZnAl or CuAlBe alloys were extensive studied by De Vos et al. (Entemeyer, 1996; De Vos et al., 1978).

The transformation strains given in (4) are deduced from the scalar g and the set of 24 vectors $\mathbf{m}^a$ and $\mathbf{n}^a$ given in the reference lattice of austenite γ. Knowing the orientation of the γ lattice with respect to the external frame, the set of the 24 transformation strains can be calculated for CuAlBe.

The knowledge of the elastic behavior and the transformation strains allow to determine completely the 24×24 terms of the interaction matrix H, whose terms are given and discussed in Appendix B. As discussed in Section 2, this matrix constitutes only a simplification (smoothing) of the real microstructure. For sake of numerical simplification or in order to take into account

additional physical phenomenon, this interaction matrix can be simplified or completed by additional terms.

The material parameters B, T_0 and the critical forces $\mathscr{F}^c$ are determined from the experiments on single crystals oriented to produce a single variant under uniaxial stress Σ_{33}. In that case the interaction term $H.f$ vanishes since $H^{mn}=0$.

During loading, austenite → martensite transformation starts with the creation of one plate of martensite, corresponding at the beginning to $f_n=0$, so $\sum_n f_n \neq 1$. Definition of Lagrange multipliers given by eqn (54a) leads to the condition $\lambda_0=0$. Transformation condition (59a) is now

$$\Sigma_{33}^{+\text{start}}\varepsilon_{33}^T - B(T-T_0) \leqslant \mathscr{F}^c \tag{71}$$

At the end of transformation, all the sample is transformed into martensite. Then $\sum_n f_n = 1$ so $f_n \neq 0$. Definition of Lagrange multipliers given by eqn (54b) leads to the condition $\lambda_n=0$. Transformation condition (59b) is now

$$\Sigma_{33}^{+\text{end}}\varepsilon_{33}^T - B(T-T_0) \geqslant \mathscr{F}^c \tag{72}$$

When transformation progresses, $\sum_n f_n \neq 1$ and $f_n \neq 0$, with only one variant active ($n=1$). These conditions lead to $\lambda_0=\lambda_n=0$, and condition for the transformation progress yields

$$\Sigma_{33}^{+}\varepsilon_{33}^T - B(T-T_0) = \mathscr{F}^c \tag{73}$$

For the reverse transformation, transformation condition (60) leads to

$$\Sigma_{33}^{-}\varepsilon_{33}^T - B(T-T_0) = -\mathscr{F}^c \tag{74}$$

Equations (73) and (74) indicate that the transformation on a single variant in a single crystal occurs at a constant stress or temperature, which is almost verified in our case (see Figs 4 and 5).

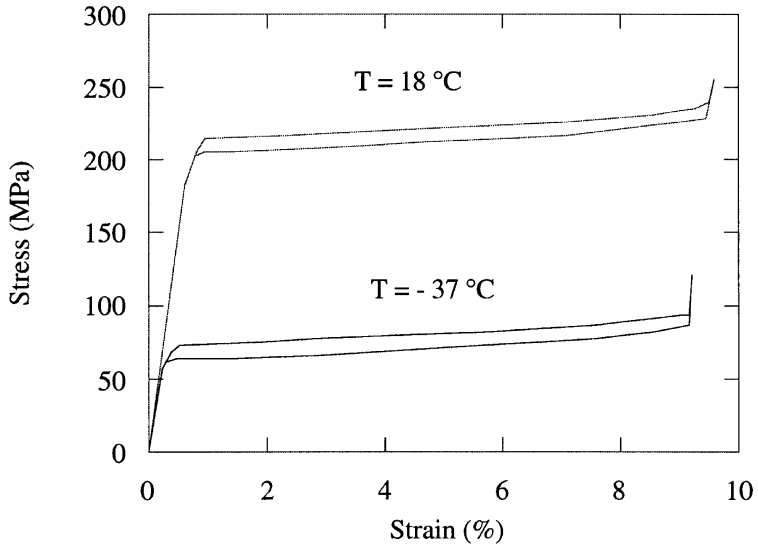

Fig. 4. Influence of a temperature change on the superelastic behavior ($T=18°C$ and $T=-37°C$) on a Cu-16 at.%Zn-15 at.%Al single crystal ($M_s=-60°C$).

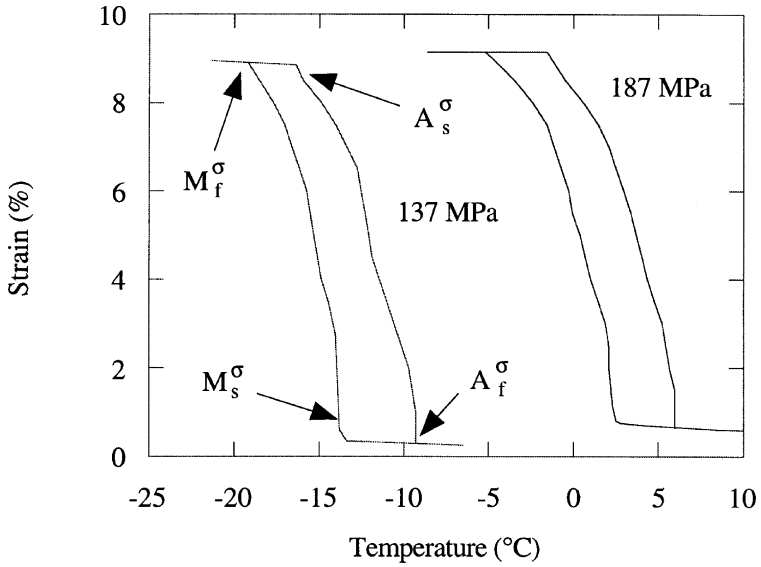

Fig. 5. Superthermal behavior of a Cu-16 at.%Zn-15 at.%Al single crystal under different constant stress level ($\sigma = 137$ Mpa and $\sigma = 187$ MPa).

A slight difference of these curves with the model corresponding to the experimental observed 'hardening' may be explained by the small strain approximation used in the model. The same phenomenon appears in the experimental results obtained during cooling at constant stress as presented in Fig. 5.

The slope of the curves $\Sigma_{33}^{+}(T)$ or $\Sigma_{33}^{-}(T)$ given by

$$\frac{\mathrm{d}\Sigma_{33}}{\mathrm{d}T} = \frac{B}{\varepsilon_{33}^{T}} \tag{75}$$

allows to find the parameter B. The hysteresis of the transformation curves leads to the critical force $\mathscr{F}^{c} = \frac{1}{2}(\Sigma_{33}^{+} - \Sigma_{33}^{-})\varepsilon_{33}^{T}$ from isothermal tests. Finally from (73) one gets the T_0 value.

Once the material parameters are found, the thermomechanical behavior of each grain of a polycrystalline SMA is given by (70) and the transformation conditions (58) and (59). These equations and material parameters can then be introduced in a self consistent scale transition scheme to get the response of the polycrystal under multiaxial thermomechanical loading conditions. This will be the aim of another paper, presented as Part II of this study about polycrystalline SMA behavior.

For the whole stress-temperature range $\{T \in [-60^{\circ}\mathrm{C}, 20^{\circ}\mathrm{C}]$ and $\Sigma_{33} \in [0, 250\ \mathrm{MPa}]\}$ martensitic start and finish temperature M_s and M_f as well as austenite start and finish temperature A_s and A_f as functions of Σ are given in Fig. 6. The quasi constant slope observed justifies the linear approximation made for the chemical energy in Section 3.

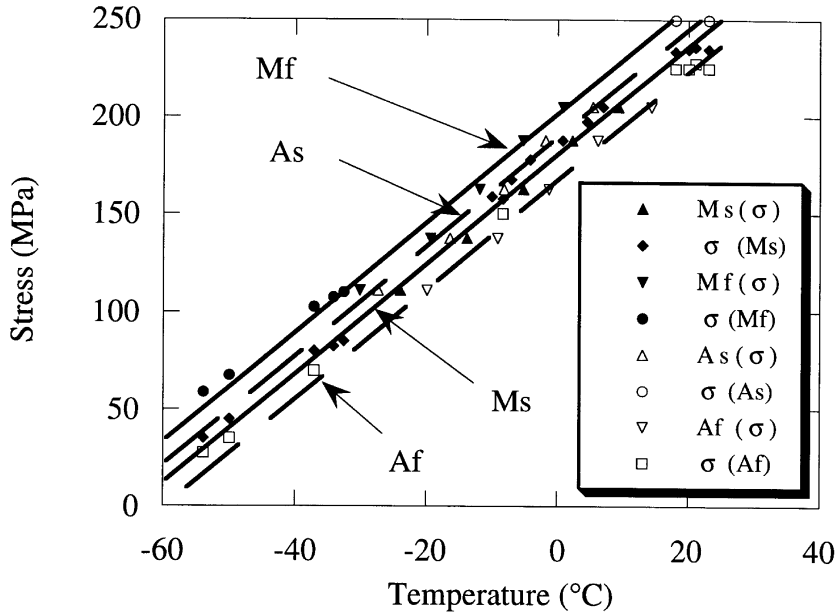

Fig. 6. State diagram experimentally defined on a Cu-16 at.%Zn-15 at.%Al single crystal from tensile tests using isothermal and anisothermal loadings. Experimental points called $\sigma(T)$ with $T = M_s$, M_f, A_s or A_f correspond to transformation stresses found during tensile tests at uniform temperatures. $T(\sigma)$ correspond to transformation temperatures found during cooling and heating at a constant level of stress.

7. Conclusions

During thermomechanical loading of shape memory alloy single crystals, only one variant is activated and the transformation progresses by displacement of plate interfaces or by creation of new plates if nucleation governs the process.

For polycrystals, the mechanism of transformation is quite different due to grain to grain as well as variant to variant interactions. These interactions induce fluctuating internal and multiaxial stresses which in turn act on the transformation pattern which corresponds to a multivariant transformation microstructure organized in domains.

While the transition from the grain level to the macroscopic one may be achieved using classical self consistent models, this paper describes the thermomechanical behavior of the grain taking into account these specific microstructures. Usual models where only the variant specific volume fractions $\{f_m\}$ or even the whole volume fraction $\{f\}$ are used as internal variables to describe the transformation microstructure are not able to take into account the spatial organization of martensitic plates observed in polycrystals. We show that the interactions between martensitic variants through the domain formation may be described by an interaction matrix depending only on the known transformation strains.

In the case of two active variants corresponding to usual situations (Entemeyer, 1996), the terms of these matrices are evaluated by the introduction of the volume fraction of domains as additional internal variables. They are calculated assuming equilibrium between domains.

The experimental determination of the material parameters introduced in the model is performed for copper-based single crystals. The terms of the interaction matrix are calculated and compared successfully with a pure compatibility condition. Classification of the variant–variant interaction is equivalent to the one well-known in physical metallurgy (El Amrani Zirifi, 1994). The results obtained from experiments and modelization, presented in this paper, are introduced into a thermomechanical self-consistent model (presented in another paper corresponding to Part II of this study). Extensive comparisons between experimental measurements on polycrystals and numerical simulation realized using these results show excellent agreement.

Appendix A

Consider an interface between two phases with the same elastic moduli C but undergoing different transformation strains ε^{in1} and ε^{in2}, respectively. As discussed by Walpole (1967) and Hill (1983), the stress and strains tensors are discontinuous across the interface, and their jumps are related together by interfacial operators. With the perfect bonding assumption, the displacement and the interfacial traction across the interface must be continuous; that is

$$[u_i] = u_i^2(r^+) - u_i^1(r^-) = 0 \tag{A1}$$

and

$$[\sigma_{ij}]n_j = (\sigma_{ij}^2(r^+) - \sigma_{ij}^1(r^-))n_j = 0 \tag{A2}$$

where n_i is the unit normal to the interface from the $(-)$ side to the $(+)$ side. At an arbitrary point $\mathbf{r}(x_i)$ of the interface, the compatibility condition $\mathrm{d}u_i = u_{i,j}\,\mathrm{d}x_j$ and the continuity of displacement along the boundary impose the relation

$$[u_{i,j}]\,\mathrm{d}x_j = 0 \tag{A3}$$

where $[x] = x^+ - x^- = x^2 - x^1$.

Since $n_i\,\mathrm{d}x_i = 0$, eqn (A3) is equivalent to

$$[u_{i,j}] = u_{i,j}^2(r^+) - u_{i,j}^1(r^-) = \lambda_i n_j \tag{A4}$$

By symmetrization the jump of strain is obtained as

$$[\varepsilon_{ij}] = \varepsilon_{ij}^2(r^+) - \varepsilon_{ij}^1(r^-) = \tfrac{1}{2}(\lambda_i n_j + \lambda_j n_i) \tag{A5}$$

λ_i is a proportionality vector which can be evaluated in terms of strain components in both sides of the interface using eqn (A2) and the following behavior:

$$\sigma_{ij}^2(r^+) = C_{ijkl}(\varepsilon_{kl}^2(r^+) - \varepsilon_{kl}^{in2}(r^+)) \tag{A6}$$

and

$$\sigma_{ij}^1(r^-) = C_{ijkl}(\varepsilon_{kl}^1(r^-) - \varepsilon_{kl}^{in1}(r^-)) \tag{A7}$$

This leads to the relation

$$[\varepsilon_{ij}] = P_{ijkl}C_{klmn}[\varepsilon_{mn}^{in}] \tag{A8}$$

where P is the interfacial operator depending on the unit normal to the interface and elastic moduli. According to Hill (1983), P has the following expression:

$$P_{ijkl} = \tfrac{1}{4}(K^{-1}_{ik} n_j n_l + K^{-1}_{jk} n_i n_l + K^{-1}_{il} n_j n_k + K^{-1}_{jl} n_i n_k) \tag{A9}$$

K^{-1} denotes the inverse to the Christoffel's matrix K defined by

$$K_{ik} = C_{ijkl} n_j n_l \tag{A10}$$

From eqns (A6)–(A8), the stress jump across the interface is given by

$$[\sigma_{ij}] = -Q_{ijkl}[\varepsilon^{\text{in}}_{kl}] \tag{A11}$$

where

$$Q_{ijkl} = (I_{ijmn} - C_{ijpq} P_{pqmn}) C_{mnkl} \tag{A12}$$

For isotropic elasticity, with Lamé constants λ and μ, Q is given by

$$Q_{ijkl} = 2\mu \left\{ F_{ijkl} + \frac{\lambda}{\lambda + 2\mu} (\delta_{ij} - n_i n_j)(\delta_{kl} - n_k n_l) \right\} \tag{A13}$$

with

$$F_{ijkl} = \tfrac{1}{2}(\delta_{ik} - n_i n_k)(\delta_{jl} - n_j n_l) + \tfrac{1}{2}(\delta_{jk} - n_j n_k)(\delta_{il} - n_i n_l) \tag{A14}$$

Appendix B: Interaction matrix for CuAlBe single crystals

For CuAlBe alloys the vectors $\mathbf{n}'$, $\mathbf{m}$ and the scalar g describing the transformation can be found in Entemeyer (1996). g is taken equal to 0.22 and the unit vectors $\mathbf{n}'^p$, $\mathbf{m}^p$ for each of the variants p ($p = 1$–24) are given in Table B1.

Concerning the mechanical properties, elastic behavior is assumed to be isotropic with Young modulus E equal to 78 GPa and Poisson's ratio equal to 0.3.

A first information about variant interactions can be deduced from pure compatibility conditions based on the incompatibility operator *Inc* (see Section 2). Applied on a piecewise uniform transformation strain $(\varepsilon^{Tp}, \varepsilon^{Tq})$ and an unknown interface normal N_k, the incompatibility tensor η is given by

$$\eta_{ij} = -\epsilon_{ikm}\epsilon_{jln}(\varepsilon^{Tp}_{mn} - \varepsilon^{Tq}_{mn}) N_k N_l \tag{B1}$$

Since compatibility means $\eta_{ij} = 0$, the equation

$$-\epsilon_{ikm}\epsilon_{jln}(\varepsilon^{Tp}_{mn} - \varepsilon^{Tq}_{mn}) N_k N_l = 0 \tag{B2}$$

has to be solved, that is to say find $\mathbf{N}$, for a given set of $(\varepsilon^{Tp}, \varepsilon^{Tq})$. The solution of eqn (B2) exists only if

$$\text{Det}(\varepsilon^{Tp}_{mn} - \varepsilon^{Tq}_{mn}) = 0 \tag{B3}$$

which is equivalent to the condition (Hill, 1980):

Table B1
Unit vectors $\mathbf{n}'^p$, $\mathbf{m}^p$ for variants p of CuAlBe alloy. The value of $\{an, bn, cn\}$ is $\{0.168, 0.688, 0.705\}$; the value of $\{am, bm, cm\}$ is $\{0.121, 0.678, 0.725\}$ (Entemeyer, 1996)

Variant p	Normal to habit plane $\mathbf{n}'$			Displacement direction $\mathbf{m}$		
1	$-an$	bn	cn	$-am$	$-cm$	bm
2	$-an$	cn	bn	$-am$	bm	$-cm$
3	an	bn	cn	am	bm	$-cm$
4	an	cn	bn	am	$-cm$	bm
5	$-bn$	$-an$	cn	cm	$-am$	bm
6	$-cn$	$-an$	bn	$-bm$	$-am$	$-cm$
7	$-bn$	an	cn	cm	am	bm
8	$-cn$	an	bn	$-bm$	am	$-cm$
9	$-an$	$-bn$	cn	$-am$	cm	bm
10	$-an$	$-cn$	bn	$-am$	$-bm$	$-cm$
11	an	$-bn$	cn	am	cm	bm
12	an	$-cn$	bn	am	$-bm$	$-cm$
13	cn	$-an$	bn	bm	$-am$	$-cm$
14	bn	$-an$	cn	$-cm$	$-am$	bm
15	cn	an	bn	bm	am	$-cm$
16	bn	an	cn	$-cm$	am	bm
17	bn	$-cn$	an	$-cm$	$-bm$	am
18	cn	$-bn$	an	bm	cm	am
19	$-bn$	cn	an	cm	bm	am
20	$-cn$	bn	an	$-bm$	$-cm$	am
21	$-cn$	$-bn$	an	$-bm$	cm	am
22	$-bn$	$-cn$	an	cm	$-bm$	am
23	cn	bn	an	bm	$-cm$	am
24	bn	cn	an	$-cm$	bm	am

$$\varepsilon_{mn}^{Tp} - \varepsilon_{mn}^{Tq} = \tfrac{1}{2}(\lambda_n N_m + \lambda_m N_n) \tag{B4}$$

where λ is a vector.

From pure kinematical considerations, one gets information about compatibility between two variants. Nevertheless eqn (B3) does not evaluate the elastic interaction if compatibility is not satisfied.

On the other hand, the matrix H^{mm} introduced in Section 4 corresponds to a quantitative description of variant–variant interactions. Due to the symmetries appearing in the transformation strain, the calculation of the determinant and of the terms of the interaction matrix have been restricted to H^{1p} and $\mathrm{Det}(\varepsilon^{T1} - \varepsilon^{Tp})$ terms ($p = 1, 24$). Table B2 presents the values obtained for $\mathrm{Det}(\varepsilon^{T1} - \varepsilon^{Tp})$ and the minimized H^{1p} terms.

For this evaluation of minimum of interaction matrix and corresponding domains interface orientation, the following numerical method has been used: testing various orientations and for a given set of them, looking for the minimum (or the minima) of corresponding interaction matrix. This was done for unit normal vectors lying in the half space $\{\langle 100\rangle, \langle 010\rangle, \langle \bar{1}00\rangle$ and

Table B2
Results of study of interacting variants $(1, p)$. Study of incompatibility by *Inc* operator or corresponding value of $\mathrm{Det}(\varepsilon^{T1} - \varepsilon^{Tp})$; comparison with the calculated minimum value of interaction matrix H^{mn} and corresponding unit normal to domains interface

Interacting variant with variant 1	$\mathrm{Det}(\varepsilon^{T1} - \varepsilon^{Tp})$	Minimum of H^{1p} (MPa)	Normal to the domain interface $\langle N_1, N_2, N_3 \rangle$		
1	0	0	—	—	—
2	0	8.79×10^{-7}	−0.1696	0.6969	0.6967
3	0	0	1	0	0
4	0	0	0	0.707	0.707
5	4.11×10^{-5}	1.22×10^{-3}	−0.727	0.685	0.056
6	2.49×10^{-3}	0.72	0.706	0.168	−0.688
7	0	0	0.707	0.707	0
8	2.41×10^{-3}	0.71	−0.706	0.168	0.688
9	0	0	0	1	0
10	7.09×10^{-5}	3.86×10^{-2}	0.121	0.725	−0.678
11	0	0	0	0	1
12	-7.09×10^{-5}	2.27×10^{-2}	−0.122	0.679	0.724
13	2.38×10^{-3}	1.06	0.121	0.725	−0.678
14	0	0	−0.707	0.707	0
15	2.44×10^{-3}	0.88	0.121	0.725	−0.678
16	-4.11×10^{-5}	1.22×10^{-3}	0.685	0.727	0.056
17	-2.44×10^{-3}	0.57	0.121	0.725	−0.678
18	7.81×10^{-6}	7.07×10^{-5}	−0.549	0.040	−0.835
19	-2.41×10^{-3}	0.39	0.122	0.727	−0.676
20	0	0	0.707	0	0.707
21	0	0	0.707	0	−0.707
22	-2.38×10^{-3}	0.55	0.121	0.725	−0.678
23	-7.81×10^{-6}	3.33×10^{-4}	−0.835	0.041	0.549
24	-2.49×10^{-3}	0.47	0.121	0.725	−0.678

$\langle 00\bar{1} \rangle, \langle 010 \rangle, \langle 001 \rangle\}$. The research had been done in seven steps. After sweeping the half space with a 20° angle step, minima are stored. For each minimum a new sweep is made with successively an 8° angle step from −20–+20° around the minimum, then a 4° angle step from −8–+8° around the new minimum. The same operation is repeated for 2, 1 and 0.5° angle steps. Finally, because it was found that some minima are very deep, value of interface orientation is precise with 0.1° step.

From values presented in Table B2, some concluding remarks may be done:

• First, one can distinguish compatible variants and incompatible variants in the sense of incompatibility operator. In the case of compatible variants, it is possible to find an interface orientation for which interaction matrix, that is to say interaction energy, is null. The involved variants are: 1, 2, 3, 4, 7, 9, 11, 14, 20 and 21. This very good agreement between incompatibility operator and interaction energy tends to prove the suitability of the thermodynamical approach of the material behavior developed in this paper.

• Moreover one can note the existence of two kinds of incompatible variants. Some of them may be called weakly incompatible variants whose interaction matrix has a low value. This is the case for variants 5, 10, 12, 16, 18, 23 for which H^{1p} is lower than 0.025 MPa. The other variants should then be designed as strongly incompatible variants with respect to variant 1. For these variants (6, 8, 13, 15, 17, 22, 24), the value of minimum of H^{1p} is higher than 0.3 MPa, that is to say at least one order of magnitude higher than the value of interaction matrix for the weakly incompatible variants. In a previous paper, Patoor et al. (1996) proposed from experimental results on Cu–Zn–Al such separation in two kinds of interaction. In the case of weak incompatible variants, they took for the interaction matrix H^{mm} about one order of magnitude lower values compared to the ones for strong incompatible variants.

Even if value of $\mathrm{Det}(\varepsilon^{T1} - \varepsilon^{Tp})$ is meaningless if different from zero, a good correlation appears between low value of this quantity and low value for interaction matrix, while the same remark can be made for high values.

• Finally, one can note the existence of preferential orientations for the interface plane. For instance, unit normal $\langle 0.121, 0.725, -0.678 \rangle$ corresponds to interface with minimum energy for many variants.

References

Abeyaratne, R., Chu, C., James, R.D., 1996. Kinetics of materials with wiggly energies: theory and application to the evolution of twinning microstructures in a Cu–Al–Ni shape memory alloy. Philosophical Magazine A 73, 457–497.

Batthacharya, K., Kohn, R.V., 1996. Symmetry, texture and the recoverable strain of shape memory polycrystals. Acta Metallurgica et Materialia 44, 529–542.

Bekker, A., Brinson, L.C., 1997. Temperature induced phase transformation in a shape memory alloy: phase diagram based kinetics approach. Journal of Mechanics and Physics of Solids 45, 949–988.

Boyd, J.G., Lagoudas, D.C., 1996. Thermodynamic constitutive model for shape memory materials—Part I: The monolithic shape memory alloy. International Journal of Plasticity 12, 805–842.

Buathier, S., 1995. Etude de la fatigue mécanique d'un monocristal CuAlBe; étude de la transformation martensitique dans un polycristal. LPMM internal report, Metz.

Christian, J.W., Olson, G.B., Cohen, M., 1995. Classification of displacive transformations: what is a martensitic transformation? Journal de Physique IV C8, 3–10.

Chu, C., James, R.D., 1995. Analysis of microstructures in Cu-14, 0%Al-3, 9%Ni by energy minimization. Journal de Physique IV C8, 143–149.

Cohen, M., Olson, G.B., Clapp, P.C., 1979. On the classification of displacive transformation (what is martensite?). Proceedings ICOMAT' 79. MIT, Cambridge, MA, pp. 1–11.

Delobelle, P., Lexcellent, C., 1996. A phenomenological three dimensional model for pseudoelastic behavior of shape memory alloys. Journal de Physique IV C1, 293–300.

De Vos, J., Aernoult, E., Delaey, L., 1978. The crystallography of the martensitic transformation of BCC into 9R: a generalized mathematical model. Zeitschrift für Metallkunde 69, 438–444.

El Amrani Zirifi, M., 1994. Contributions à l'étude micromécanique des transformations martensitiques thermoélastiques. Ph.D. thesis. Université de Metz, Metz, France.

Entemeyer, D., 1996. Etude micromécanique du comportement thermomécanique des alliages à mémoire de forme. Ph.D. thesis, Université de Metz, Metz, France.

Entemeyer, D., Patoor, E., Eberhardt, A., Berveiller, M., 1995. Micromechanical modelling of the superthermoelastic behavior of materials undergoing thermoelastic phase transition. Journal de Physique IV C8, 233–238.

Falk, F., 1980. Model free energy, mechanics, and thermodynamics of shape memory alloys. Acta Metallurgica 28, 1773–1780.

Grujicic, M., Olson, G.B., Owen, W.S., 1985. Mobility of the $\beta_1 - \gamma_1'$ martensitic interface in Cu–Al–Ni: Part I. Experimental measurements. Metallurgical Transactions A 16A, 1723–1734.

Hill, R., 1983. Interfacial operators in the mechanics of composite media. Journal of Mechanics and Physics of Solids 31, 347–357.

Krishnan, R.J., Delaey, L., Tas, H., Warlimont, H., 1974. Review. Thermoelasticity, pseudoelasticity and the memory effects associated with martensitic transformations. Journal of Materials Science 9, 1536–1544.

Kröner, E., 1980. Physics of Defects. North-Holland, Amsterdam.

Leclercq, S., Lexcellent, C., 1996. A general macroscopic description of thermomechanical behavior of shape memory alloys. Journal of Mechanics and Physics of Solids 44, 953–980.

Lipinski, P., Berveiller, M., 1989. Elastoplasticity of micro-inhomogeneous metals at large strains. International Journal of Plasticity 5, 149–172.

Müller, I., Xu, H., 1991. On the pseudo-elastic hysteresis. Acta Metallurgica et Materialia 39, 263–271.

Mura, T., 1993. Micromechanics of Defects in Solids. Kluwer Academic, Dordrecht, The Netherlands.

Patoor, E., Berveiller, M., 1997. CISM Courses and Lecture No. 368: Mechanics of Solids with Phase Changes. Springer, Wien, NY.

Patoor, E., Eberhardt, A., Berveiller, M., 1987. Potentiel pseudoélastique et plasticité de transformation martensitique dans les mono-et polycristaux métalliques. Acta Metallurgica 35, 2779–2789.

Patoor, E., Eberhardt, A., Berveiller, M., 1996. Micromechanical modelling of superelasticity in shape memory alloys. Journal de Physique IV C1, 277–292.

Peyroux, R., Chrysochoos, A., Licht, C., Löbel, M., 1996. Phenomenological constitutive equations for numerical simulations of SMA's structures. Journal de Physique IV C1, 347–356.

Raniecki, B., Lexcellent, C., 1994. R_L-models of pseudoelasticity and their specification for some shape memory solids. European Journal of Mechanics A, Solids 13, 21–50.

Rice, J.R., 1971. Inelastic constitutive relations for solids: an internal variable theory and its application to metal plasticity. Journal of the Mechanics and Physics of Solids 19, 433–455.

Sittner, P., Takakura, M., Hara, Y., Tokuda, M., 1996. On transformation pathways of general stress controlled thermoelastic martensitic transformation in shape memory alloys. Journal de Physique IV C1, 357–366.

Stalmans, R., Van Humbeeck, J., Delaey, L., 1995. Thermodynamic modelling of shape memory behavior: some examples. Journal de Physique IV C8, 203–208.

Sun, Q.P., Hwang, K.C., 1991. A micromechanics constitutive model of transformation plasticity with shear and dilatation effect. Journal of the Mechanics and Physics of Solids 39, 507–524.

Sun, Q.P., Hwang, K.C., 1994. Micromechanics constitutive description of thermoelastic martensitic transformations. Advances in Applied Mechanics 41, 249–298.

Sun, Q.P., Lexcellent, C., 1996. On the unified micromechanics constitutive description of one-way and two-way shape memory effects. Journal de Physique IV C1, 367–376.

Tanaka, K., Kobayashi, S., Sato, Y., 1986. Thermomechanics of transformation pseudoelasticity and shape memory effect in alloys. International Journal of Plasticity 2, 59–72.

Walpole, L.J., 1967. The elastic field of an inclusion in an anisotropic medium. Proceedings of the Royal Society, Series A 300, 270–289.

Warlimont, H., 1976. Shape memory effects. Materials Science and Engineering 25, 139–144.

Weschler, M.S., Lieberman, D.S., Read, T.A., 1953. On the theory of the formation of martensite. Transactions of AIME 197, 1503–1515.

Wollants, P., De Bonte, M., Roos, J.R., 1979. A thermodynamic analysis of the stress-induced martensitic transformation in a single crystal. Zeitschrift für Metallkunde 70, 113–117.